Available online at www.sciencedirect.com
ScienceDirect
International Journal of Mass Spectrometry 266 (2007) 76–85
International Journal of Mass Spectrometry
www.elsevier.com/locate/ijms

Differential mobility spectrometer: Model of operation

E.V. Krylov *, E.G. Nazarov, R.A. Miller

Sionex Corp., 8-A Preston Court, Bedford, MA 01730, USA

Received 4 May 2007; received in revised form 13 July 2007; accepted 13 July 2007
Available online 19 July 2007

Abstract

Differential mobility spectrometry is a powerful tool used in a rapidly growing number and variety of applications for detection and characterization of gas-phase ions. In this paper a comprehensive mathematical model of the apparatus implementing the differential mobility spectrometry method is described. For completeness the mathematical theory of the method is provided. The model focuses on the analytical parameters of the differential mobility spectrometry instrument. The influence of instrumental parameters (carrier gas flow rate, separating field amplitude and waveform, filter gap size and geometry) and ion properties (diffusion, mobility and electric field mobility dependence) on the spectral peak characteristics (position, height and width) is examined. Both planar and coaxial instruments are covered in the same mathematical model. The model is extensively validated using published and our own experimental data. Proposed model is demonstrated to be in a good quantitative agreement with experimental data. This model explains all observed phenomena and predicts new ones such as high field focusing.

Keywords: Differential mobility spectrometer; FAIMS; Spectral peak; Modeling

The method of the differential mobility spectrometry proposed in Refs. [1–3] has been recognized as a powerful tool for separation and characterization of gas-phase ions. Ions are distinguished by the difference between mobilities at high and low electric fields due to the fact that ion mobility values depend on the applied field strength. The method is easy to use, sensitive, fast and relatively selective. Developed and refined over the past decade differential mobility spectrometry has become topical. Many publications on this theme have appeared recently. The method of differential mobility spectrometry is also known as field ion spectrometry (FIS) [4] and field-asymmetric waveform ion mobility spectrometry (FAIMS) [5]. Two main types of apparatus embodiments are distinguished by planar and coaxial geometries of the ion filter gap. Both planar and coaxial geometries have been implemented in commercial products: planar SVAC (Sionex, Bedford, MA) and coaxial Selectra (ThermoElectron, Waltham, MA), with the number and diversity of applications growing rapidly.

Since performance of the differential mobility spectrometry apparatus depends significantly on the implementation, modeling of the instrument operation is important. There are two main approaches to the operation modeling: mathematical [6–8] and computational [9,10]. Some authors argue for importance of the computational modeling over the mathematical. In our opinion these approaches are not competitive but rather complimentary. Each has own advantages and drawbacks so they should be used together. Mathematical modeling is mostly for understanding the general principles and trends. Computational modeling is for detailed quantitative calculations.

The present paper focuses on mathematical modeling of the operation of the differential mobility spectrometry apparatus. We begin with a review the general principles of differential mobility spectrometry. Then we propose an operational model for the differential mobility spectrometry apparatus based on the solution of the ion diffusion equation inside the filter gap. The model is significantly extended in comparison with previous publication [7]. Then we examine the spectral peak depending on the instrumental parameters. And finally, we compare predicted characteristics and experimental data.

1. Principles of operation

In order to examine the instrumental model of operation it is essential to clarify the principles of operation. This section provides a general description of the differential mobility

* Corresponding author. Tel.: +1 781 457 5373; fax: +1 781 275 2135.
E-mail address: ekrylov@sionex.com (E.V. Krylov).

1387-3806/$ – see front matter © 2007 Elsevier B.V. All rights reserved.
doi:10.1016/j.ijms.2007.07.003

spectrometry method and mathematical representation of the phenomena involved.

1.1. General notions

An electric field of strength E causes trace amounts of ion to move through a dilute gas media of density N. The velocity of the ions drift is known to be proportional to the parameter E/N through the coefficient of mobility, K. If the energy the ion gains from the electric field is small enough in comparison with the thermal energy, K is a constant and independent of E/N. But with increasing values of E/N the mobility coefficient becomes dependent on the electric field as shown in Eq. (1):

$$K\left(\frac{E}{N}\right) = K(0)\left[1 + \alpha\left(\frac{E}{N}\right)\right], \quad (1)$$

where $K(0)$ is the mobility coefficient under low field conditions; $\alpha(E/N) \ll 1$ is normalized function describing field-mobility dependence (called alpha dependence below); E/N is the electric field in Townsend ($1\,\mathrm{Td} = 10^{-17}\,\mathrm{V\,cm^2}$) units. Under normal conditions ($N_0 = 2.687 \times 10^{19}\,\mathrm{cm^{-3}}$) 1 Td corresponds to 268.7 V/cm.

Fig. 1a shows examples of various field-mobility dependencies derived from published experimental data [11–18] for the positive and negative ions from a ^{63}Ni source in air under conditions near the normal (temperature 300–500 K; atmospheric pressure). The data had been cross-checked and found to be consistent. Since negative ions move against the electric field their mobility coefficients are considered negative. Corresponding alpha dependencies for these ions are presented in Fig. 1b. Low field mobilities and alpha dependencies of these ions will be used below for quantitative comparison of the model and experiment.

The alpha dependence may be approximated as an even power series of the electric field strength. That polynomial form is supported by symmetry considerations [19] (i.e., an ion velocity value doesn't depend on the electric field direction).

$$K\left(\frac{E}{N}\right) = K(0)\left[1 + \alpha_2\left(\frac{E}{N}\right)^2 + \alpha_4\left(\frac{E}{N}\right)^4 + \cdots\right], \quad (2)$$

where $\alpha_2, \alpha_4, \ldots, \alpha_{2n}$ are series coefficients of the alpha dependence expansion. Series coefficients are definitively related to the corresponding alpha dependence. The number and values of the series coefficients may vary to fit experimental accuracy. It is important to emphasize here that there is no physical meaning behind the expansion coefficients. The power series expansion is a just convenient mathematical expression for the alpha function.

The alpha dependence is a unique feature of ion utilized for the ions separation in differential mobility spectrometry. The method of differential mobility spectrometry is implemented by a flowing of the gas stream containing ions through a gap between two electrodes (called the "filter gap") as shown in Fig. 2.

A high amplitude, high frequency, asymmetric waveform (called separation voltage, SV) is applied to the electrodes to create an electric field (called separation field, S) affecting the ions. The ions undergo fast oscillations in response to this separation field. The displacements during the positive and negative half-period of the waveform differ slightly because of unequal mobilities at the high and low fields. As a result of this displacement ions drift in a perpendicular direction to the gas flow, toward one of the electrodes. Ions pass through the gap between the electrodes only if the transverse drift velocity is zero. Drifting ions eventually reach one of the electrodes and neutralize. The ion's drift velocity and direction depend on the separation field amplitude, waveform, and alpha dependence.

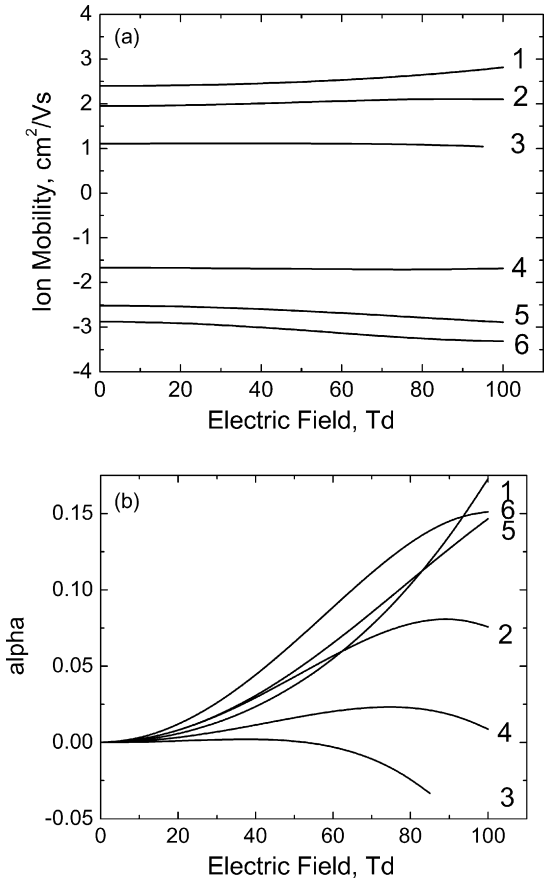

Fig. 1. (a) Field-mobility dependence and (b) normalized field-mobility dependence for positive and negative ions in air under conditions near the normal. Curves are numerated as follows: (1) positive reactant ions in purified air identified as protonated water cluster $H^+(H_2O)_n$; (2) protonated monomer of dimethyl methyl phosphonate, H^+(DMMP) (125 Da); (3) proton bound dimer of dimethyl methyl phosphonate, $H^+(DMMP)_2$ (249 Da); (4) deprotonated 2,4-dinitrotoluene ions $(DNT\text{-}H)^-$ (181 Da); (5) negative reactant ions in purified air identified as $O_2^-(H_2O)_n$; (6) chlorine ions Cl^- (35 Da).

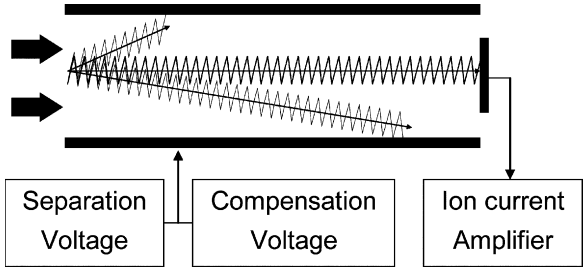

Fig. 2. Instrumental implementation of the differential mobility spectrometry.

Particular ions may be restored to the center of the gap (i.e., compensated, with no net drift) by applying a low strength constant compensation voltage (CV) to the electrodes. The constant electric field (called compensation field, C) is superimposed on the separation field, and produces an offsetting drift, allowing ions to remain in equilibrium inside the gap. Ions with differing drift velocities, due to their properties, can be passed through the gap at different compensation voltages. Scanning the CV produces a spectrum of the ionic mixture. Differential mobility spectrometry apparatus is called a differential mobility spectrometer (DMS).

1.2. Mathematical description

The electric field between the DMS electrodes is

$$E(t) = Sf(t) + C, \tag{3}$$

where $E(t)$ is the applied electric field; C is the compensation field; $S \gg C$ is the amplitude of the separation field; $f(t)$ is a function describing field waveform.

The separation field in a differential mobility spectrometer must be such that its average value over a period is zero (zero offset condition) while the amplitude of positive half-period is not equal to the negative half-period (asymmetry condition).

$$\langle f \rangle \equiv \frac{1}{T}\int_0^T f(t)\mathrm{d}t = 0, \quad \langle f^3 \rangle \equiv \frac{1}{T}\int_0^T f^3(t)\mathrm{d}t \neq 0, \tag{4}$$

where T is the period of the separation field; triangular brackets denote the averaging over the period of the separation field.

Under the action of this field ions oscillate and drift perpendicular to the carrier gas flow toward the electrodes. The average ion drift velocity may be written as:

$$\langle \upsilon(t) \rangle = \left\langle K\left(\frac{E}{N}\right)(Sf(t) + C)\right\rangle. \tag{5}$$

Only ions with average velocity equal zero pass through the gap. To solve for C Eq. (1) is substituted into Eq. (5) and it is equated to zero [3].

$$\langle (1+\alpha)(Sf + C)\rangle = 0, \tag{6}$$

Expanding alpha function by Taylor's theorem in terms of the small parameter C/S yields a first order approximation for the compensation field C.

$$C = \frac{S\langle \alpha f\rangle}{1 + \langle \alpha\rangle + S\langle \alpha' f\rangle}, \tag{7}$$

where C is the absolute value of the compensation field; S is the amplitude of the separation field; $f(t)$ is the waveform; α is the alpha dependence and α' is the derivative with respect to E/N; triangular brackets denote the average over a period of the separation field.

Thus, knowing the alpha dependence, the waveform $f(t)$, and the amplitude of the separation field S, one can calculate the compensation field for certain ions. The inverse problem also can be solved: knowing the experimental dependence $C(S)$, one can calculate the alpha dependence. A detailed procedure to do this will be described.

When ions are separated in a spatially inhomogeneous (coaxial or spherical) electric field, the field strength, and hence the ion drift velocity become position dependent. It had been found [2,20] that under certain conditions the ion-focusing effect appears, effectively decreasing the diffusion losses of the ion transmission. This means that the ions diffusing along the field lines from the point of equilibrium (point where the compensation condition is fulfilled) are exposed to a restoring force. In other words, under the action of the spatially inhomogeneous electric field, the ions start drifting toward the point of equilibrium. In the linear approximation, drift velocity, V_{focus}, is

$$V_{\mathrm{focus}} = K\left(C - \frac{\mathrm{d}C}{\mathrm{d}S}S\right)\frac{\nabla E}{E(r_0)}\Delta r \equiv \gamma \cdot \Delta r, \tag{8}$$

where $E(r_0)$ is the electric field at the point of equilibrium; ∇E is the field gradient; γ is the focusing factor; C is the compensation field; S is the separation field amplitude and Δr is the small displacement from the position of equilibrium. For the coaxial filter gap the focusing factor is

$$\gamma = \frac{K}{\rho}\left(C - \frac{\mathrm{d}C}{\mathrm{d}S}S\right), \tag{9}$$

where C is the compensation field; S is the separation field amplitude; K is the ion mobility and ρ is the median radius of the filter gap. The necessary condition for ion focusing is a negative sign of the focusing factor, otherwise de-focusing takes place. In that case the ions drift from the point of equilibrium toward the walls.

2. Model of operation

This section describes the main considerations for a mathematical model of the operation of the differential mobility spectrometer. First we will examine ion distribution in the DMS filter gap. Then we will apply the solution to the investigation of the DMS spectral peak. Finally we will discuss the model's restrictions and limitations.

The DMS provides information about analyzed ion mixture in a spectral form. A spectral peak can be characterized by its position, height and width. These characteristics depend on the many factors. Influencing the DMS peak are instrumental parameters such as carrier gas flow rate, separating field amplitude and waveform, filter gap sizes and geometry. Ion properties such as diffusion, mobility and alpha dependencies also affect the DMS peak characteristics. To sort out these relations, we must consider DMS operation in detail.

Physically the DMS signal is an ion current measured at the output of the filter gap (see Fig. 2). This current is a product of averaged ion density and carrier gas flow rate. Instrumental parameters and ion properties affect the ion density and hence the output current. Thus, to find DMS peak characteristics requires us to know the ion density distribution in the DMS filter gap.

2.1. Ion density distribution

According to Fick' second law ion density distribution is given by a solution of three-dimensional time-dependent diffusion equation with some boundary conditions.

$$\frac{\partial n}{\partial t} + \nabla(-D\nabla n + nV) = 0, \tag{10}$$

where n is the ion density; V is the ion drift velocity and D is the ion diffusion. This equation is too complex to solve without some simplifying assumptions. Therefore, we make the following assumptions:

(1) The DMS spectral peak is a well-resolved peak corresponding to stable ions (no ion-molecular reactions and/or ion transformations are taken into consideration).
(2) Effects of gas velocity distribution and ion diffusion in the carrier gas flow direction are assumed to be negligible. Gas flow is supposed to be laminar.
(3) The geometry and surface of the filter gap are assumed to be ideal.
(4) An electric field, which affects ions in the filter gap results in the following:
   (a) The diffusion and mobility coefficients become dependent on the field strength and are connected by the generalized Einstein's relation [19]. The diffusion becomes anisotropic i.e., dependent on the electric field direction. Longitudinal (along the field) diffusion coefficient, D_L, may be significantly larger then tangential (across the field) diffusion coefficient D_T.
   (b) The effective gap, g, between electrodes is smaller then the physical gap because the ions need enough space to oscillate with the SV without striking the electrodes.

$$g = d - \frac{SK}{2F}\langle|f|\rangle. \tag{11}$$

   In this equation, K is the ion mobility; S is the separation field amplitude; F is the separation field frequency; f is the separation field waveform and d is the distance between the electrodes (filter gap).
   (c) Transversal ion velocity is assumed to be equal to $K\Delta C$, where ΔC is a small deviations of the compensation field near the value of compensation ($\Delta C = 0$ corresponds to the condition of compensation for this ion).
   (d) Spatial field gradient results in the ion drift with a velocity equal to the product of the ion displacement from the point of equilibrium and the focusing factor γ given by the Eq. (9).

Under these assumptions, ion density distribution in the filter gap may be found as a solution of one-dimensional, time-dependent, diffusion equitation with zero boundary conditions.

$$\frac{\partial n}{\partial t} + \frac{\partial}{\partial x}\left(-D_L\frac{\partial n}{\partial x} + \gamma n x + K\Delta C n\right) = 0 \quad n(\pm g/2) = 0, \tag{12}$$

where n is the ion density; D is the coefficient of diffusion; x is the coordinate along the electric field; γ is the focusing factor; $K\Delta C$ is the small uncompensated ion drift velocity and g is the effective gap.

In assumption of independent variables (so-called τ-approximation) solution is sought in the form

$$n(x;t) = n_0(x)\exp\left(-\frac{t}{\tau}\right). \tag{13}$$

The spatial part of the solution, $n_0(x)$, describes the established profile of the ion density in the filter gap. The time part of the solution determines the ion losses in the filter gap. In the τ-approximation Eq. (12) reduces to the time-independent diffusion equation with zero boundary conditions

$$-Dn_0'' + n_0'(\gamma x + K\Delta C) + n_0(\gamma - \tau^{-1}) = 0 \quad n_0\left(\pm\frac{g}{2}\right) = 0. \tag{14}$$

We must now consider particular cases of the ion focusing.

2.1.1. Weak focusing

The focusing effects is negligible in comparison with diffusion. This case corresponds to the DMS filter gap with a planar geometry. In this case Eqs. (13) and (14) provide an accurate solution.

$$|\gamma| \ll \frac{D}{g^2} \quad n(x;t) = \cos\left(\frac{\pi x}{g}\right)\exp\left(\frac{K\Delta C x}{2D}\right) \times \exp\left\{-t\left(\frac{D\pi^2}{g^2} + \frac{(K\Delta C)^2}{4D}\right)\right\}. \tag{15}$$

Under the condition of compensation ($\Delta C = 0$) the ion density has a cosinusoidal profile and decays exponentially. The decay constant depends on the diffusion coefficient and the effective gap.

2.1.2. Intermediate focusing

Diffusion and focusing effects are comparable. This is a typical condition for the coaxial DMS. If $\Delta C \neq 0$ the Eq. (14) has no analytical solution. Under the condition of compensation ($\Delta C = 0$) the solution is

$$|\gamma| \sim \frac{D}{g^2}, \quad n(x;t) = n_0(x)\exp\left\{-t\frac{D\pi^2}{g^2}\exp\left(\frac{g^2\gamma}{2\pi^2 D}\right)\right\}. \tag{16}$$

where D is the coefficient of diffusion; γ is the focusing factor; g is the effective gap.

The decay constant now depends on the focusing factor as well as the diffusion coefficient and effective gap. Notice that Eqs. (16) and (15) are consistent: if $\gamma = 0$ and $\Delta C = 0$ their time parts are the same. An analytical solution for the spatial ion density distribution doesn't exist but it may be estimated as

$$n_0(x) \approx \exp\left(\frac{\gamma x^2}{2D}\right)\cos\left(\frac{\pi x}{g}\right). \tag{17}$$

2.1.3. Strong focusing

In this case diffusion is negligible compared with the focusing effect. This corresponds to a high focusing factor and high separation field. In the case of focusing ($\gamma < 0$), the ion density has a Gaussian profile and does not change in time.

$$|\gamma| \gg \frac{D}{g^2} \quad n_0(x) = \exp\left(\frac{\gamma x^2}{2D}\right). \tag{18}$$

The diffusion coefficient and focusing factor define the characteristic size of the ion cloud

$$\sigma = \sqrt{\frac{2D}{|\gamma|}} \ll g. \tag{19}$$

The solutions of the diffusion equation in the DMS filter gap, allows analytical calculations of the DMS peak characteristics.

2.2. The DMS spectral peak

The DMS spectral peak is characterized by its position, height and width. We will begin from the peak position because it is the most accurate part of the model. Then we will examine DMS peak height based on the concept of the ion transmission coefficient. And finally the peak width expression will be derived as a particular case of non-compensated ion transmission.

2.2.1. Peak position

The DMS peak position is determined by the ion field mobility dependence and separation field amplitude and waveform Eq. (7). For practical purposes it may be simplified significantly by a series expansion [3]. The compensation field may be written as an expansion

$$C(S) = c_3 S^3 + c_5 S^5 + c_7 S^7 + \cdots, \tag{20}$$

and field mobility dependence (alpha dependence) as an expansion

$$\alpha(E) = \alpha_2 E^2 + \alpha_4 E^4 + \alpha_6 E^6 + \cdots. \tag{21}$$

Substituting into Eq. (7) we obtain the coefficients c_{2n+1}

$$c_3 = \alpha_2\langle f^3\rangle \qquad c_5 = \alpha_4\langle f^5\rangle - 3c_3\alpha_2\langle f^2\rangle$$
$$c_7 = \alpha_6\langle f^7\rangle - 5c_3\alpha_4\langle f^4\rangle - 3c_5\alpha_2\langle f^2\rangle, \tag{22}$$

where the separation waveform coefficients by definition are

$$\langle f^n\rangle = \frac{1}{T}\int_0^T f^n(t)\mathrm{d}t. \tag{23}$$

The separation waveform coefficients for real separation voltage generators [21] are presented in the Table 1.

The compensation field plotted against the separation field amplitude (half sinusoidal waveform) for various ions is shown in Fig. 3a. Electric field units (Td) may be recalculated into Volts for particular implementation of the DMS for direct comparison with raw DMS data. But we recommend *E*/*N* scaling as a standardized presentation of the DMS spectra, which enables comparison of the spectra obtained for different pressures [22] and even for various sensor designs (will be discussed below).

Table 1
Separation waveform coefficients

Waveform	$\langle f^2\rangle$	$\langle f^3\rangle$	$\langle f^2\rangle$	
Rectangular (ideal)	0.512	0.269	0.330	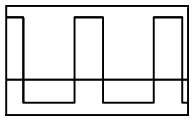
Two harmonics	0.310	0.110	0.120	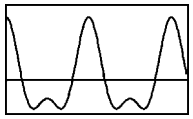
Half sinusoidal	0.236	0.111	0.103	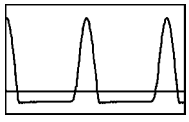

Power series expansion allows solution of the inverse problem, the alpha dependence calculation. Since Eq. (22) is reversible, the alpha dependence for certain ions may be reconstructed from the experimental data. Approximating the experimental dependence $C(S)$ as an expansion into a series of odd powers of the separation field, S, and knowing the separation

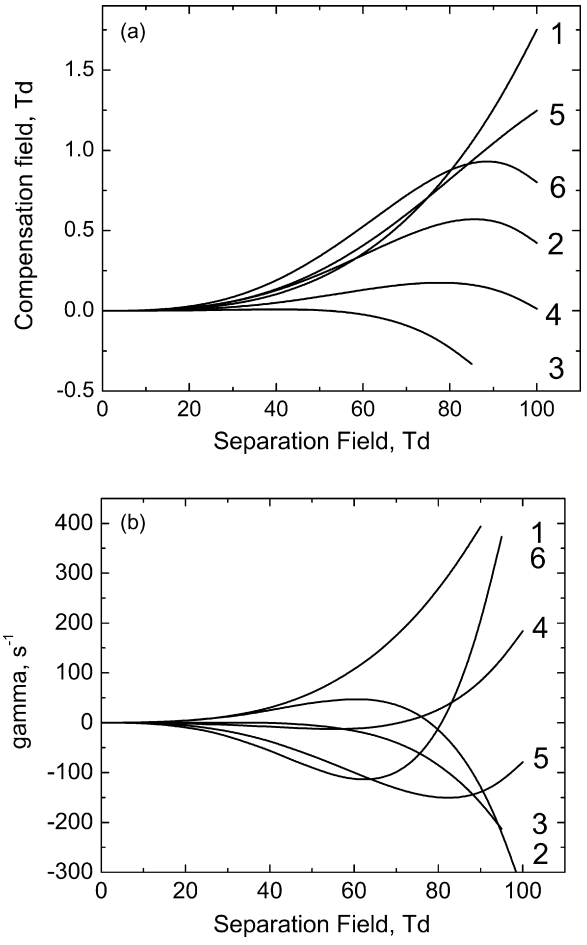

Fig. 3. (a) Compensation field and (b) focusing factor as a function of separation field amplitude for the positive and negative ions in air. (1), $H^+(H_2O)_n$; (2), $H^+(DMMP)$; (3), $H^+(DMMP)_2$; (4), $(DNT\text{-}H)^-$; (5), $O_2^-(H_2O)_n$ and (6), Cl^-.

waveform, one can obtain the expansion of the alpha function into a series of even powers of the electric field [3,23].

2.2.2. Peak height

The concept of the ion transmission through the filter gap is used to calculate the DMS peak height. We define the ion transmission coefficient, L, as a ratio of integral ion densities at the input and output of the filter gap. An ion transmission coefficient equal to zero corresponds to total ions loss (no output ion current); an ion transmission coefficient equal to 1 corresponds to lossless passage through the DMS filter gap. Since the spatial ion density profile is supposed to be the same along the DMS filter gap (τ-approximation), the time part of the diffusion equation solution gives the expression for the ion transmission coefficient

$$L = \exp\left(-\frac{t_{res}}{\tau}\right), \quad (24)$$

where t_{res} is the residence time (the time an ion spends in the DMS filter gap); τ is the coefficient of exponential decay. Both the residence time, and the coefficient of exponential decay depend on the DMS parameters. The DMS peak height and peak width may be derived from the ion transmission coefficient.

The DMS peak height, H, by definition is the output ion current under the compensation condition. Ion current is a product of the averaged by cross section input ion concentration, n_{in}, carrier gas flow rate, Q, and the ion transmission coefficient. According to Eq. (16) the DMS peak height is given by

$$H = n_{in} Q \exp\left\{-t_{res}\frac{\pi^2 D}{g^2}\exp\left(\frac{g^2\gamma}{2\pi^2 D}\right)\right\}, \quad (25)$$

where D is the ion diffusion; γ is the focusing factor; Q is the DMS carrier gas flow rate; g is the effective gap; t_{res} is the residence time.

For the planar DMS peak height expression Eq. (25) can be simplified because the focusing factor is zero. Nonzero focusing factor corresponds to DMS separation in spatially inhomogeneous (coaxial or spherical) electric field. Sign and value of the focusing factor Eq. (9) depend on the ion properties (polarity, mobility and alpha function), and separation field amplitude and inhomogeneity (median radius of the filter gap for coaxial DMS). Knowing the compensation field expansion Eq. (20) we can derive the focusing factor as odd power series.

$$\gamma(S) = \frac{K}{\rho}(2c_3 S^3 + 4c_5 S^5 + 6c_7 S^7 + \cdots), \quad (26)$$

Focusing factors for some ions plotted against the separation field amplitude are shown in Fig. 3b. For the calculation we assumed a two harmonics waveform and a 0.8 cm filter gap median radius.

Now we have all we need for peak height calculation. Ion transmission coefficients (proportional to the peak heights) for three ion species plotted against the separation field amplitude are presented on the Fig. 4. Solid curves correspond to the coaxial DMS (median radius is 0.8 cm), dotted – to the planar DMS. Other calculation parameters were the same: two harmonics waveform, frequency of 0.25 MHz, the residence time of 0.27 s, the filter gap of 0.2 cm.

The ion transmission coefficient, and consequently peak height, significantly varies with the separation field amplitude and polarity, especially for the coaxial DMS. The planar DMS exhibits an overall monotonic behavior. The peak height decreases with increasing the separation field independently of the ion type and/or field polarity. The rule of thumb is the higher the ion mobility the greater the ion losses in the filter gap.

The coaxial DMS behavior differs as it was investigated in detail in Ref. [7]. Using the concept of the focusing factor we can explain and predict peak height behavior in the coaxial DMS. Ion transmission without the separation field is the same as for the planar DMS since residence time and gap are the same. The positive separation field (Fig. 4b) results in the focusing for negative ions (increasing peak height) and defocusing for positive ions (decreasing peak height). At higher separation field strength the peak height decreases for negative ions as well. A negative separation field leads to the inverse situation, i.e., peak height increases for positive ions and decreases for negative (Fig. 4a).

This is consistent with what is known about DMS focusing effect. Our model not only explains known phenomena but also predicts new one. According to the model some ions (such as DMMP ions) are focused at high separation field (rising branch of the curve 2 in the Fig. 4b). Low positive separation field

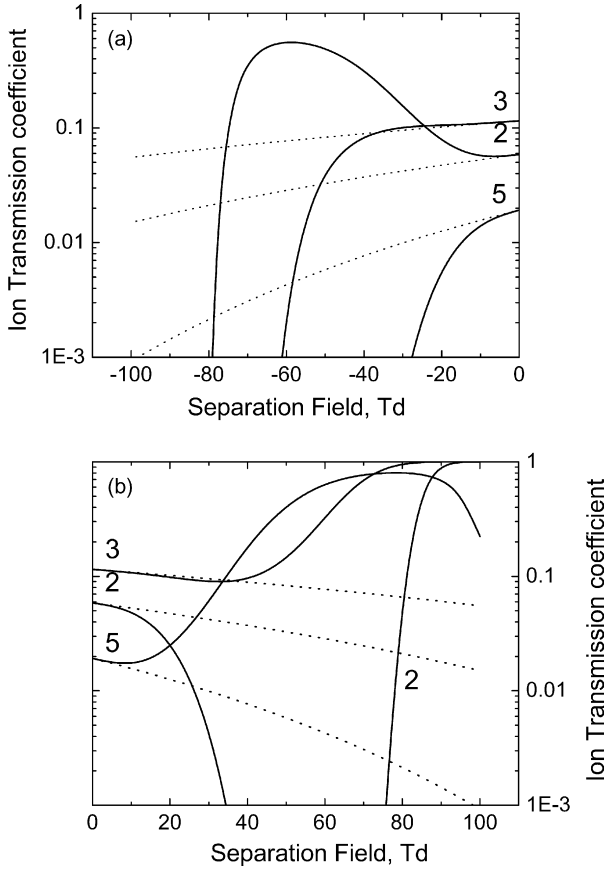

Fig. 4. Ion transmission coefficient (proportional to the peak height) vs. negative (a) and positive (b) separation field for coaxial DMS (solid curves) and planar DMS (dotted curves). Positive and negative ions in air: 2, $H^+(DMMP)$; 3, $H^+(DMMP)_2$ and 5, $O_2^-(H_2O)_n$.

results in the defocusing effect for positive DMMP ions. So peak height for these ions vanishes. But at higher separation fields the focusing factor for DMMP ions changes sign (see Fig. 3b) resulting in the focusing and peak height increasing. Defocusing changing by focusing at high separation field is still not verified experimentally. The phenomenon of high field focusing may constitute a test of our model validity.

2.2.3. Peak width

Varying the compensation field near the compensation condition for certain ions decreases the ion transmission and forms the DMS peak. At certain value of the compensation field deviation, ΔC, the output ion current reduces by half. In the framework of the ion transmission concept, the peak width W at half maximum is given by

$$L\left(\Delta C = \frac{W}{2}\right) = \frac{L(\Delta C = 0)}{2}, \tag{27}$$

where ΔC is a small deviation from the compensation condition.

Let us consider the cases of weak (planar DMS), strong and intermediate (coaxial DMS) focusing separately.

2.2.4. Weak focusing

Ion density distribution in the filter gap is significantly non-stationary if the gas flow rate is sufficiently high and the residence time is much less then the characteristic diffusion time. It means that the effect of the diffusion is negligible. Equating the ion displacement during the residence time to the effective gap [24] yields the DMS peak width neglecting the diffusion

$$W_1 = \frac{g}{Kt_{\text{res}}}, \tag{28}$$

where K is the coefficient of mobility; W_1 is the DMS peak width at half maximum; g is the effective gap and t_{res} is the residence time.

The case of low gas flow rate is characterized by a residence time much greater than the characteristic diffusion time and may be considered as quasi-stationary. The peak width may be found from the solution of the diffusion equation in the DMS filter gap. Substituting Eq. (15) into Eq. (27) gives the expression for the peak width

$$W_2 = \frac{4}{K}\sqrt{\frac{\ln 2D}{t_{\text{res}}}}, \tag{29}$$

where K is the coefficient of mobility; D is the diffusion coefficient; W_2 is the DMS peak width at half maximum; g is the effective gap and t_{res} is the residence time.

2.2.5. Strong focusing

When the ion cloud of characteristic size σ (see Eq. (19)) is within the filter gap there are no ion losses (coefficient of the ion transmission $L = 1$). Deviation of the compensation field results in a displacement of the center of the ion cloud to a distance

$$\Delta x = \frac{K\Delta C}{\gamma} = \frac{\Delta C\rho}{(C - C'S)}. \tag{30}$$

where K is the coefficient of mobility; S is the separation field amplitude; C is the compensation field; ΔC is the deviation of the compensation field and γ is the focusing factor.

If the ion cloud center displacement is such that ion cloud touches the wall, ion losses rise drastically. A strongly focused DMS peak has a flat top (actually the peak top will be sloped because of different conditions near the inner and outer walls of the coaxial filter gap) and his width is given by

$$W_3 = \frac{(g - a\sigma)|\gamma|}{K}, \tag{31}$$

where K is the coefficient of mobility; $a \sim 3$ is a numerical coefficient; γ is focusing factor; σ is the characteristic size of the ion cloud; g is effective gap and W_3 is DMS peak width at half maximum.

2.2.6. Intermediate focusing

Eq. (14) has no analytical solution for $\gamma \neq 0$ and $\Delta C \neq 0$. Nevertheless the ion transmission function for this case, $L_1(\Delta C)$, may be found based on the known ion transmission function $L(g)$ as follows.

Let us examine the ion density distribution in the coaxial filter gap (g) near the compensation condition ($\Delta C \neq 0$). In this case, the ion density distribution becomes asymmetrical. The asymmetry means that the ion density maximum shifts away from the center of the gap. In a first approximation the shift value, Δx, is given by Eq. (30). The ion density distribution on one side from the maximum is the same as for the wide gap of $g + 2\Delta x$. And the ion density distribution on the other side of the maximum is the same as for the narrow gap of $g - 2\Delta x$. The function $L_1(\Delta C)$ may be written as

$$L_1(\Delta C) = \sqrt{L(g + 2\Delta x)L(g - 2\Delta x)}, \tag{32}$$

This function provides a general solution for the DMS peak shape for a wide range of the DMS parameters.

2.3. Model restrictions

Any physical model has some restrictions and limitations. A clear understanding of them is important for the model to be relevant. Here we briefly overview the restrictions and limitations of the proposed model.

Main limitation of the model is the assumption of independent variables (τ-approximation). The ion density profile is supposed to be steady along the filter gap. It means that all kinds of transient phenomena are neglected. These phenomena include all transitions and irregularities along the ion flow path. Usually transitions and irregularities lead to additional ion losses (decreasing peak height). So the model gives an upper limit of the DMS performance.

Strictly speaking the process of the ion focusing also may be considered as a transition to another ion distribution. The criteria for the model applicability is given in the relation between the characteristic focusing time, which may be estimated as inverse focusing factor, γ^{-1}, and the residence time t_{res}. If for a particular coaxial DMS the focusing time is much less than the residence

time, the proposed model works well. Otherwise there is no focusing effect and this DMS should be considered planar.

The DMS instrument (including the filter gap geometry, surfaces quality, etc.) is assumed to be ideal. Since real instruments are inherently non-ideal, their parameters may vary from the predicted ones. Non-ideality may be taken into account as a small disturbance. By applying the correction terms the model accuracy for non-ideal instruments can be improved significantly.

The space charge field may affect the DMS performance if the ion density is significant. Ions are repulsed by the space charge field toward the filter gap walls hence ion losses raise. However under typical operating conditions the space charge effect is negligible, as verified by modeling using computational methods [25] too.

Surface charging and fringe field effects are also not considered in this model.

Nevertheless as we will see below in the most of practically important situations proposed model gives a good quantitative agreement with the experimental data.

3. Experimental

The DMS technique became topical in the past few years. A lot of experimental data had been published and discussed. These data as well as our own experiments provide material to test the model. The following examples are meant to illustrate the proposed model's validity. The main idea here is to take experimental data and model them under the same experimental conditions. Correlation between the theoretical curves and experimental data points will constitute a test of the model's validity.

3.1. DMS peak position

Ion properties (alpha dependence) and separation voltage parameters (amplitude and waveform) affect the DMS peak position (compensation voltage). Here we are going to calculate the compensation voltage, CV, in dependence on the separation voltage amplitude, SV, for the same ions but different DMS instruments (planar and coaxial).

Positive reactant ions identified as $(H_2O)_nH^+$ was chosen for the validation. The alpha dependence for these ions is shown in Fig. 1b.

Experimental data for the planar DMS was obtained with SVAC (Sionex Corporation, Bedford, MA). Experimental parameters were: the filter gap of 0.05 cm; the separation voltage amplitude in the 500–1500 V range; half sinusoidal waveform (see Table 1); gas temperature of 30 °C.

Experimental data for the coaxial DMS, who referred as FAIMS in the article, was derived from Ref. [9]. Experimental parameters were: the filter gap of 0.2 cm; the separation voltage amplitude (DV in the article) in the 1800–2600 V range; two harmonics waveform (see Table 1); gas temperature of 25 °C.

Following the procedure described above we plotted positive reactant ion peak positions (compensation voltage) against the separation voltage amplitude. Good agreement with experimental data was observed for both planar and coaxial instruments (see Fig. 5).

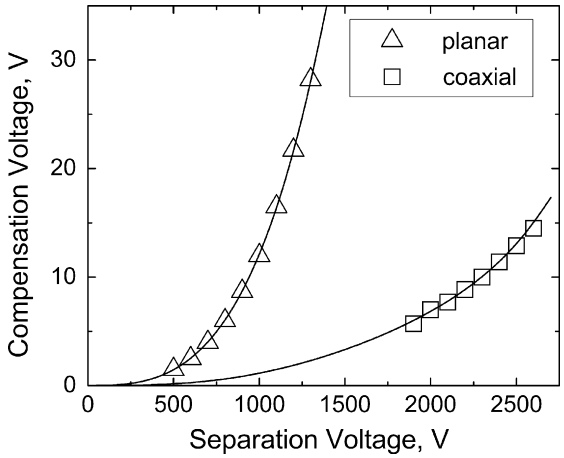

Fig. 5. Positive reactant ion (protonated water clusters $(H_2O)_nH^+$) peak position dependence on the separation voltage amplitude (SV). Experimental data was acquired with coaxial (squares) and planar (triangles) DMS instruments. The experiments are compared with theoretical predictions (solid curves) based on the known alpha function and instrumental parameters (filter gap and separation field).

Thus, knowing the alpha dependence and instrumental parameters allows the peak position to be calculated for different DMS instruments. From other side, alpha dependence determined from the experiments with different DMS instruments appears to be the same. As an example, compare the alpha functions for $(DNT\text{-}H)^-$ ions reported in Refs. [14,15]. Even though very different raw data was obtained from different DMS units, it resulted in the same alpha dependence. This means that the alpha function is a substantially dependent on the ion type and independent on the instrumental implementation.

3.2. DMS peak height

The DMS peak height depends on many parameters but the most significant influences are the separation field and the gas flow rate. Here we are going to examine the gas flow dependence for the planar DMS, and the separation field dependence for the coaxial DMS.

Experimental data for the planar DMS was obtained with the instrument described in Ref. [26]. The parameters were: DMS filter gap of 0.05 cm; length of 1.5 cm; width of 0.4 cm; the separation voltage amplitude of 800 V; frequency of 1.3 MHz; half sinusoidal waveform. Carrier gas flow rate in the 3–17 cm^3/s range; gas temperature of 50 °C. Negative reactant ions in purified air, $O_2^-(H_2O)_n$, were chosen for the validation. The alpha dependence for these ions is shown in Fig. 1b. Fig. 6 shows a good correlation between the theoretical curve and experimental points. The high flow discrepancy may be explained by saturation of the ion source.

Experimental data for the coaxial DMS (ion drift nonlinearity spectrometer in the article) was published in Ref. [27]. Experimental parameters were: DMS filter gap of 0.16 cm; length of 7 cm; median radius of 0.42 cm; the separation voltage amplitude in the 1700–3600 V range; frequency of 0.17 MHz; half

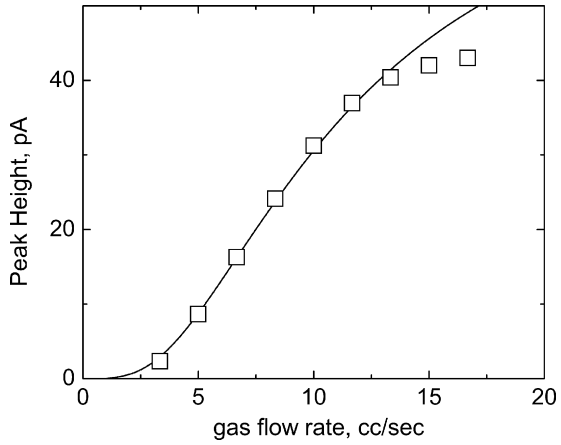

Fig. 6. Shows the planar DMS peak intensity as a function of the carrier gas flow rate for negative reactant ions in purified air, $O_2^-(H_2O)_n$. The experimental data is compared with theoretical predictions (solid curves) for a DMS with filter gap = 0.05 cm; length = 1.5 cm; width = 0.4 cm; separation voltage amplitude = 800 V; carrier gas temperature = 50 °C.

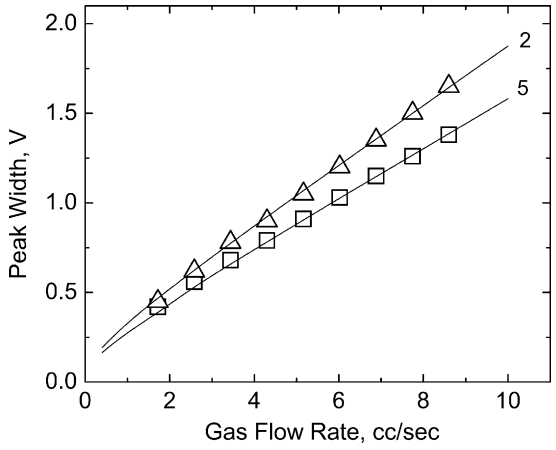

Fig. 8. Planar DMS peak width vs. gas flow rate for H^+(DMMP) ions (curve 2, theory, triangles – experiment) and for $O_2^-(H_2O)_n$ ions (curve 5, theory, squares – experiment).

sinusoidal waveform; carrier gas flow rate of 50 cm^3/s; gas temperature of 120 °C. Negative ions of the 2,4-dinitrotoluene i.e., deprotonated molecular ions $(DNT\text{-}H)^-$ were chosen for the model validation. The alpha function for these ions is shown in Fig. 1b. Fig. 7 exhibits a good correlation between the theoretical curve and the experimental data.

3.3. DMS peak width

The DMS peak width (full width at half maximum) appears to be strongly dependent on the gas flow rate for the planar DMS and on the separation voltage amplitude for the coaxial DMS. The foregoing examples were chosen to illustrate this as well as the validity of our model.

Dependence of the DMS peak width on the gas flow rate was obtained with the planar DMS (SVAC, Sionex Corporation Bedford, MA). The ions under investigation were: negative reactant ions in purified air, $O_2^-(H_2O)_n$ and protonated monomers of dimethyl methyl phosphonate, H^+(DMMP). Instrumental parameters were: DMS filter gap of 0.05 cm; length of 1.5 cm; width of 0.1 cm; gas flow rate in the 1–8 cm^3/s range; the separation voltage frequency of 1.18 MHz; half sinusoidal waveform; amplitude of 1000 V. Experimental points, squares for negative RIP and triangles for DMMP ions, lie on the theoretical curves as shown in Fig. 8.

DMS peak width plotted against the separation voltage amplitude for the coaxial DMS is shown in Fig. 9. The peak corresponds to the positive reactant ions identified as $(H_2O)_nH^+$. Alpha dependence for these ions is presented in Fig. 1b. Experimental data was derived from Ref. [9]. The DMS parameters were: the filter gap of 0.2 cm; median radius of 0.8 cm; length of 9 cm; the residence time of 0.27 s; the separation field frequency of 0.25 MHz; two harmonics waveform; amplitude in the 1800–2600 V range. We modeled this dependence under two conditions, a strong (Eq. (31), dotted curve) and intermediate (Eq. (32), solid curve) focusing effect. Both conditions result in

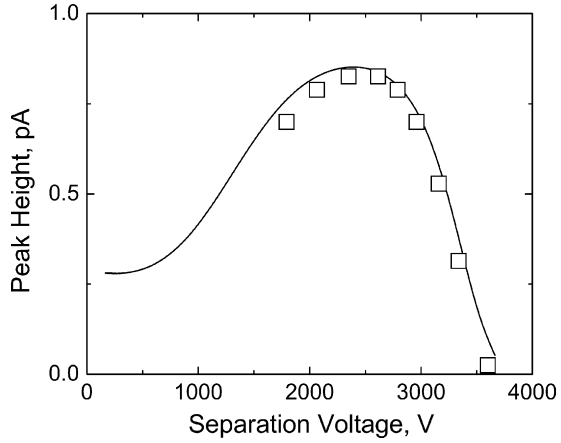

Fig. 7. Comparison of experimental (squares) and theoretical (solid curves) data showing the coaxial DMS peak intensity as a function of the applied separation voltage amplitude for 2,4-dinitrotoluene ions $(DNT\text{-}H)^-$. DMS filter gap is 0.16 cm; length is 7 cm; median radius is 0.42 cm; carrier gas flow rate is 50 cm^3/s; temperature is 120 °C.

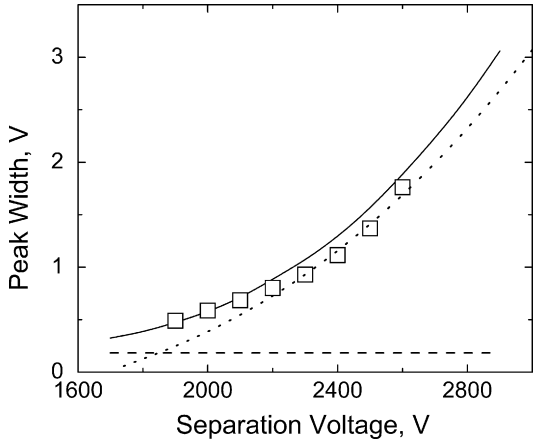

Fig. 9. Coaxial DMS peak width as a function of separation voltage for the positive reactant ion peak (protonated water clusters $(H_2O)_nH^+$). Experimental data (squares) are compared with the models at strong (dotted curve) and intermediate (solid curve) focusing. The peak width for the planar DMS (dashed curve) is provided for reference.

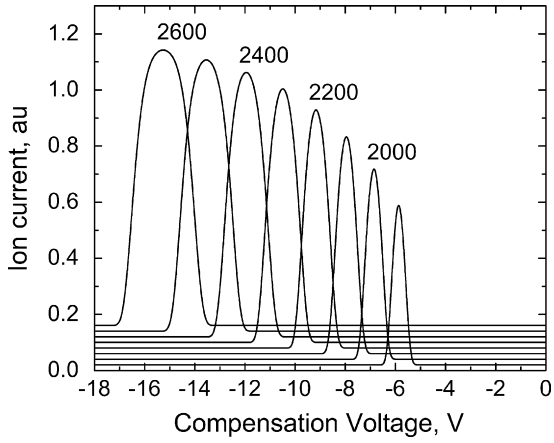

Fig. 10. Modeling of the positive reactant ion peak profile for the coaxial DMS at various separation voltages (frequency is 0.25 MHz; two harmonics waveform; residence time is 0.27 s; filter gap is 0.2 cm; median radius is 0.8 cm).

the theoretical curve agrees satisfactorily with the experimental data.

The planar DMS exhibits very weak peak width dependence on separation voltage amplitude. It follows from the Eq. (28) and has been confirmed experimentally. The calculated dependence (dashed curve in Fig. 9) corresponds to the planar DMS with the same parameters as the coaxial DMS. Thus, mathematical modeling shows that increasing the DMS curvature (or decreasing median radius of coaxial electrodes) significantly increases DMS peak width. This is consistent with the results of Ref. [25].

Eq. (32) provides not only the peak width but also the peak shape similar to the one observed experimentally. E.g., compare modeled DMS peak in Fig. 10 with real coaxial DMS spectra shown in Fig. 3 of Ref. [9]. The calculation parameters were the same as the experimental ones: positive reactant ion ($H^+(H_2O)_n$); frequency of 0.25 MHz; two harmonics waveform; residence time of 0.27 s; gap of 0.2 cm; median radius of 0.8 cm. Our model accurately predicts the coaxial DMS peak shape transformation with the increasing the separation voltage, from quasi-triangular to quasi-sinusoidal and eventually to quasi-rectangular.

4. Conclusions

A comprehensive mathematical model is proposed for the differential mobility spectrometer. Proposed model quantitatively describes the dependence of the DMS spectral peak characteristics (height, width and position) on the DMS instrumental parameters (carrier gas flow rate, amplitude and form of the separating field, geometry of the filter gap) and the ion characteristics (diffusion, mobility and field mobility dependence). The model shows a good qualitative and quantitative agreement with experimental data over a wide range of experimental conditions. The phenomenon of high field focusing is predicted. Proposed model can be utilized for the optimization and prediction of the DMS analytical parameters. On the whole, this mathematical model of the DMS operation advances our understanding of differential mobility spectrometry.

Acknowledgement

The authors wish to thank Dr. Stephen Coy (Sionex Corporation Inc., Bedford, MA) for numerous discussions.

References

[1] M.P. Gorshkov, Inventor's Certificate of USSR No.966583, G01N27/62, 1982.
[2] I.A. Buryakov, E.V. Krylov, V.P. Soldatov, Inventor's Certificate of USSR No. 1485808, G01N27/62, 1989.
[3] I.A. Buryakov, E.V. Krylov, E.G. Nazarov, U.Kh. Rasulev, Int. J. Mass Spectrom. Ion Proc. 128 (1993) 143.
[4] B. Carnahan, S. Day, V. Kouznetsov, M. Matyjaszczuk, A. Tarassov, Proceeding of the International Conference on Advance in Instrumentation and Control ISA, 1996, pp. 87–95.
[5] R.W. Purves, R. Guevremont, S. Day, C.W. Pipich, M.S. Matyjaszczyk, Rev. Sci. Instrum. 69 (1998) 4094.
[6] E.V. Krylov, PhD Thesis. (1995), St.-Petersburg Polytechnic University, Russia.
[7] E.V. Krylov, Int. J. Mass Spectrom. 225 (2003) 39.
[8] I.A. Buryakov, Tech. Phys. 51 (2006) 1121.
[9] R. Guevremont, R.W. Purves, Rev. Sci. Instrum. 70 (1999) 1370.
[10] A.A. Shvartsburg, K. Tang, R.D. Smith, J. Am. Soc. Mass Spectrom. 15 (2004) 1487.
[11] P. Kebarle, in: B.E. Conway, J.O'M. Bockris (Eds.), Modern Aspects of Electrochemistry, vol. 9, Plenum Press, New York, 1974.
[12] P. Kebarle, Ann. Rev. Phys. Chem. 28 (1977) 445.
[13] N. Krylova, E. Krylov, G.A. Eiceman, J.A. Stone, J. Phys. Chem. A 107 (2003) 3648.
[14] G.A. Eiceman, E. Krylov, N. Krylova, E.G. Nazarov, R.A. Miller, Anal. Chem. 76 (2004) 4937.
[15] I.A. Buryakov, Talanta 61 (2003) 369.
[16] T.W. Carr, Anal. Chem. 51 (1979) 705.
[17] H. Bohringer, D.W. Fahey, W. Lindinger, F. Howorka, F.C. Fehsenfeld, D.L. Albritton, Int. J. Mass Spectrom. Ion Process. 81 (1987) 81.
[18] L.A. Viehland, E.A. Mason, Atom. Data Nucl. Data Tables 60 (1995) 37.
[19] E.A. Mason, E.W. McDaniel, Transport Properties of Ions in Gases, Wiley, New York, 1988.
[20] E.V. Krylov, Tech. Phys. 44 (1999) 113–116.
[21] E.V. Krylov, Instrum. Exp. Tech. 40 (1997) 628.
[22] E.G. Nazarov, S.L. Coy, E.V. Krylov, R.A. Miller, G.A. Eiceman, Anal. Chem. 78 (2006) 7697.
[23] E. Krylov, E.G. Nazarov, R.A. Miller, B. Tadjikov, G.A. Eiceman, J. Phys. Chem. A. 106 (2002) 5437.
[24] I.A. Buryakov, E.V. Krylov, V.P. Soldatov, in: V.V. Malakhov (Ed.), Chemical Analysis of Environment, Nauka, Novosibirsk, 1991, p. 113.
[25] A.A. Shvartsburg, F. Li, K. Tang, R.D. Smith, Anal. Chem. 78 (2006) 3706.
[26] G.A. Eiceman, E.V. Krylov, B. Tadjikov, R.G. Ewing, E.G. Nazarov, R.A. Miller, Analyst 129 (2004) 297.
[27] I.A. Buryakov, Yu.N. Kolomiets, B.V. Luppu, J. Anal. Chem. 56 (2001) 336.